AIAA JOURNAL
Vol. 49, No. 8, August 2011

Characterization and Constitutive Modeling of Composite Materials Under Static and Dynamic Loading

Isaac M. Daniel,* Jeong-Min Cho, Brian T. Werner, and Joel S. Fenner
Northwestern University, Evanston, Illinois 60208

DOI: 10.2514/1.J050797

Composite materials were characterized under quasi-static and dynamic loading, and a constitutive model was proposed to describe the nonlinear multi-axial behavior of the materials at varying strain rates. The material investigated was a unidirectional carbon-fiber/epoxy composite. Multi-axial experiments were conducted at three strain rates, quasi-static (10^{-4} s^{-1}), intermediate (1 s^{-1}), and high (180–400 s^{-1}), using offaxis specimens to produce stress states combining transverse normal and in-plane shear stresses to verify the model. A Hopkinson-bar apparatus and offaxis specimens loaded in this system were used for multi-axial characterization of the material at high strain rates. Stress–strain curves under tension and compression were obtained for various loading orientations with respect to the fiber direction. A nonlinear constitutive model is proposed following an elastic–plastic approach. It is based on a potential function in the form of a linear combination of deviatoric and dilatational deformation components. The model is able to describe the rate-dependent behavior under multi-axial states of stress including tensile and compressive loading. Experimental results were in good agreement with predictions of the proposed constitutive model.

Nomenclature

A	=	constant
a_1, a_2, a_4, a_6	=	plastic anisotropy parameters
b_1, b_2	=	plastic anisotropy parameters
C_{ij}	=	stiffness matrix components, Pa
dW_p	=	incremental plastic strain energy per unit volume, Pa
$d\gamma_6^p$	=	plastic shear strain increment on 1-2 plane
$d\varepsilon_i$	=	total strain increment
$d\bar{\varepsilon}_p$	=	effective plastic strain increment
$d\varepsilon_i^e$	=	elastic strain increment
$d\varepsilon_i^p$	=	plastic strain increment
$d\varepsilon_x^p$	=	plastic strain increment along loading direction
$d\lambda$	=	scalar function of proportionality
$d\sigma_j$	=	stress increment, Pa
f	=	plastic potential function
S_{ij}	=	compliance matrix components, Pa^{-1}
ε_x^p	=	plastic strain along x axis (loading direction)
$\bar{\varepsilon}_p$	=	effective plastic strain
η	=	constant
θ	=	angle between loading and fiber directions
μ	=	elastic anisotropy parameter
σ_i	=	normal stress components, Pa
$\bar{\sigma}_e$	=	effective stress, Pa
σ_x	=	axial stress (along loading direction), Pa
$\sigma_1, \sigma_2, \sigma_3$	=	normal stress components along principal material axes, Pa
τ_4, τ_5, τ_6	=	shear stress components on 2-3, 1-3, and 1-2 principal planes, Pa

Presented at the 51st AIAA/ASME/ASCE/AHS/ASC Structures, Structural Dynamics, and Materials Conference, Orlando, FL, 12–15 April 2010; received 16 August 2010; revision received 17 March 2011; accepted for publication 27 March 2011.

*Center for Intelligent Processing of Composites, McCormick School of Engineering and Applied Science; imdaniel@northwestern.edu.

I. Introduction

THE ever-expanding applications of composite materials expose them to severe loading and environmental conditions and pose new challenges to the designer. In many structural applications composite materials are exposed to high energy, high velocity dynamic loadings producing multi-axial dynamic states of stress. Under these conditions composites exhibit nonlinear and rate-dependent behavior. Nonlinear behavior arises primarily from plastic deformation of the polymeric matrix and is especially pronounced when shear components are dominant in the state of stress. Therefore, it is important to characterize experimentally the nonlinear dynamic behavior of composites under multi-axial states of stress and describe their behavior by appropriate constitutive models.

Many test methods have been developed and discussed for characterization of composite materials at various strain rates [1–13]. Quasi-static and low strain rates up to approximately 10 s^{-1} are obtained in a servohydraulic testing machine; strain rates between 10 s^{-1} and approximately 200 s^{-1} have been generated using an instrumented drop-tower apparatus; and higher rates up to and exceeding 1000 s^{-1} are produced by means of a split Hopkinson (or Kolsky) pressure bar [6–12]. Most of the high-rate studies deal with uniaxial compression. In a few cases uniaxial tensile test methods have been described, e.g., Daniel et al. [1] and Gilat et al. [12]. These studies have shown considerable increases in stiffness and strength with strain rate. In some cases, explicit empirical relations were given for the rate dependence of these mechanical properties [7,10]. Most of the reported work to date deals with a one-dimensional state of stress, i.e., uniaxial compression, tension, or shear. Hsiao et al. [7], Ninan et al. [11], and Vinson and Woldesenbet [10] determined the dynamic behavior under combined compression and shear by testing unidirectional offaxis specimen in a Hopkinson-bar apparatus. The compressive and shear stress–strain behavior was determined independently of each other as a function of strain rate. Bing and Sun [13] tested offaxis specimens by the Hopkinson-bar technique and developed a model to extract the compressive strength of the material as a function of strain rate. Modeling the nonlinear behavior observed in the tests above is a challenging task.

For quasi-static loading, Sun and Chen [14] and Gates and Sun [15] proposed a one-parameter plasticity model based on a Hill-type [16] quadratic plastic potential, by assuming a plane-stress state and no plastic deformation in the fiber direction. The parameter in the potential function was determined from uniaxial offaxis tests. This model has been widely accepted and its accuracy and range of applicability were investigated and reported in [17]. Chen and Sun

[18] later proposed a quadratic plastic potential function independent of dilatational deformation, by introducing elastic anisotropic parameters that are defined as the ratios of elastic constants along the principal material directions. More recently, Yokozeki et al. [19], pointed out that one-parameter constitutive models are not fully capable of describing the nonlinear mechanical behavior under tension or compression loading combined with shear loading, unless their anisotropic parameters are obtained separately in the tension and compression regimes. This is due to the fact that polymer composites display dilatation-dependent mechanical behavior not captured in the quadratic yield (plastic potential) function used. Yokozeki et al. extended Sun and Chen's [14] model and proposed a two-parameter model that distinguishes between tension and compression of the plastic flow in composite materials under monotonic loading. One of the parameters accounts for the anisotropic behavior and the other distinguishes the sign of the normal stress. Yokozeki et al. [19] employed the approach of Drucker and Prager's [20] plasticity model and expanded Sun and Chen's [14] model by adding a hydrostatic term. However, in order to maintain the hydrostatic term in their model, they allowed plastic deformation in the fiber direction.

The models above did not include strain-rate effects. Thiruppukuzhi and Sun [21,22] and Weeks and Sun [23] extended the one-parameter model to account for rate effects as well. They introduced two additional parameters obtained by curve-fitting a power law function to the effective plastic strain determined by offaxis tests at different strain rates. Goldberg and Stouffer [24] proposed a strain-rate-dependent viscoplastic model using a micromechanics analysis and used Hashin's stress criteria for failure prediction based on given strength properties. Zhu et al. [25] extended this model by a numerical procedure to account for the transverse shear effects. Xing and Reifsnider [26] proposed a three-parameter constitutive model representing large nonlinear deformation and rate-dependent behavior under tension. Donadon et al. [27] proposed a three-dimensional viscoplastic constitutive model incorporating strain-rate effects. Model validation was done by comparing measured and predicted uniaxial stress–strain curves. Elastic-viscoplastic constitutive models, like the ones described above, can describe the rate-dependent material behavior with emphasis on large inelastic deformations. They make use of several parameters that must be determined by fitting to experimental data.

In the research described in the present paper, composite materials are characterized under quasi-static and dynamic multi-axial states of stress. A new nonlinear constitutive model is proposed to describe their rate-dependent behavior under states of stress including tensile and compressive loading. The proposed potential function consists of a linear combination of deviatoric and dilatational deformation components. Experimental results were in good agreement with predictions of the proposed constitutive model.

II. Material Characterization

The material investigated was a carbon/epoxy composite (AS4/3501-6) obtained in prepreg form and used for preparation of laminates by the standard autoclave process. Multi-axial experiments were performed by testing unidirectional carbon/epoxy specimens at various loading directions with respect to the principal fiber reinforcement. These experiments produced primarily stress states combining transverse normal and in-plane shear stresses. Two to six specimens were tested in each case.

Experiments were conducted at three strain rates. Quasi-static tests were conducted in a servohydraulic testing machine at a strain rate of 10^{-4} s^{-1}. Intermediate-rate tests were also conducted in the servohydraulic machine at an average strain rate of 1 s^{-1}. A special fixture was designed with a gap between the specimen and the bottom crosshead to allow for crosshead acceleration up to a nearly uniform speed before the load was transferred to the specimen, thus ensuring a more uniform strain rate during the test (Fig. 1). High-strain-rate tests were conducted by means of a split Hopkinson pressure bar at strain rates ranging from 180 to 400 s^{-1} using prismatic offaxis specimens (Fig. 2).

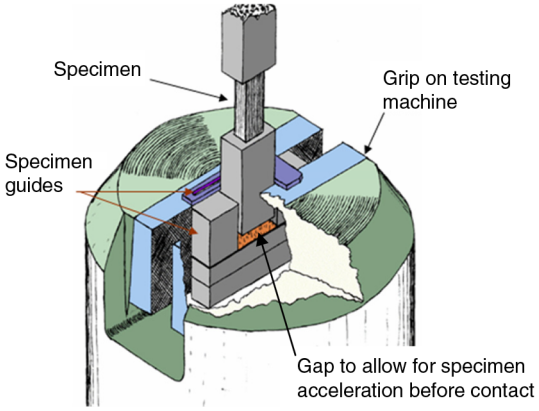

Fig. 1 Compression testing at intermediate strain rates.

Multi-axial static and dynamic experiments were conducted using offaxis specimens to produce stress states combining transverse normal and in-plane shear stresses. Figure 3 shows typical static and dynamic stress–strain curves for the unidirectional carbon/epoxy composite for various loading orientations at three strain rates: quasi-static, intermediate, and high. The intermediate-rate curves correspond to an average strain rate of 1 s^{-1}, and the high-rate curves correspond to rates in the range of 180–400 s^{-1}.

III. Constitutive Modeling

An element of a unidirectional composite under load along the principal material axes is shown in Fig. 4. In the general nonlinear elastic–plastic stress–strain response illustrated in Fig. 5, the total strain increment corresponding to an increment in stress can be decomposed into an elastic and a plastic part as

$$d\varepsilon_i = d\varepsilon_i^e + d\varepsilon_i^p \tag{1}$$

The plastic strain increment is related to a potential (or loading) function through the associated flow rule and normality rule as follows:

$$d\varepsilon_i^p = d\lambda \frac{\partial f}{\partial \sigma_i} \tag{2}$$

where $i = 1, 2, \ldots, 6$; f is a plastic potential function; and $d\lambda$ is a scalar function of proportionality. The constitutive model sought is obtained from the plastic potential and scalar functions.

A plastic potential function was proposed based on a modified Drucker–Prager [20] yield criterion consisting of deviatoric and

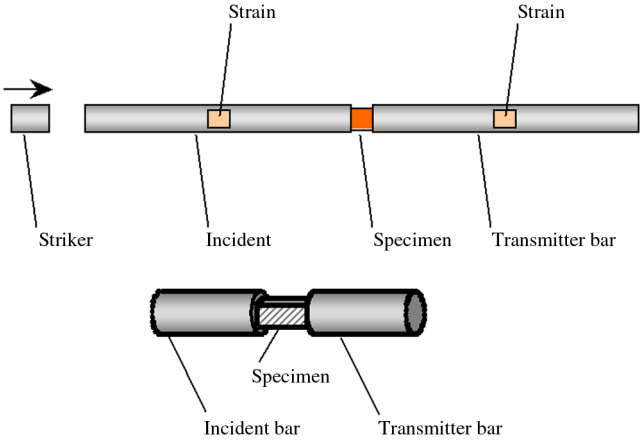

Fig. 2 Hopkinson bar and offaxis specimen used for high-rate testing of carbon/epoxy composites.

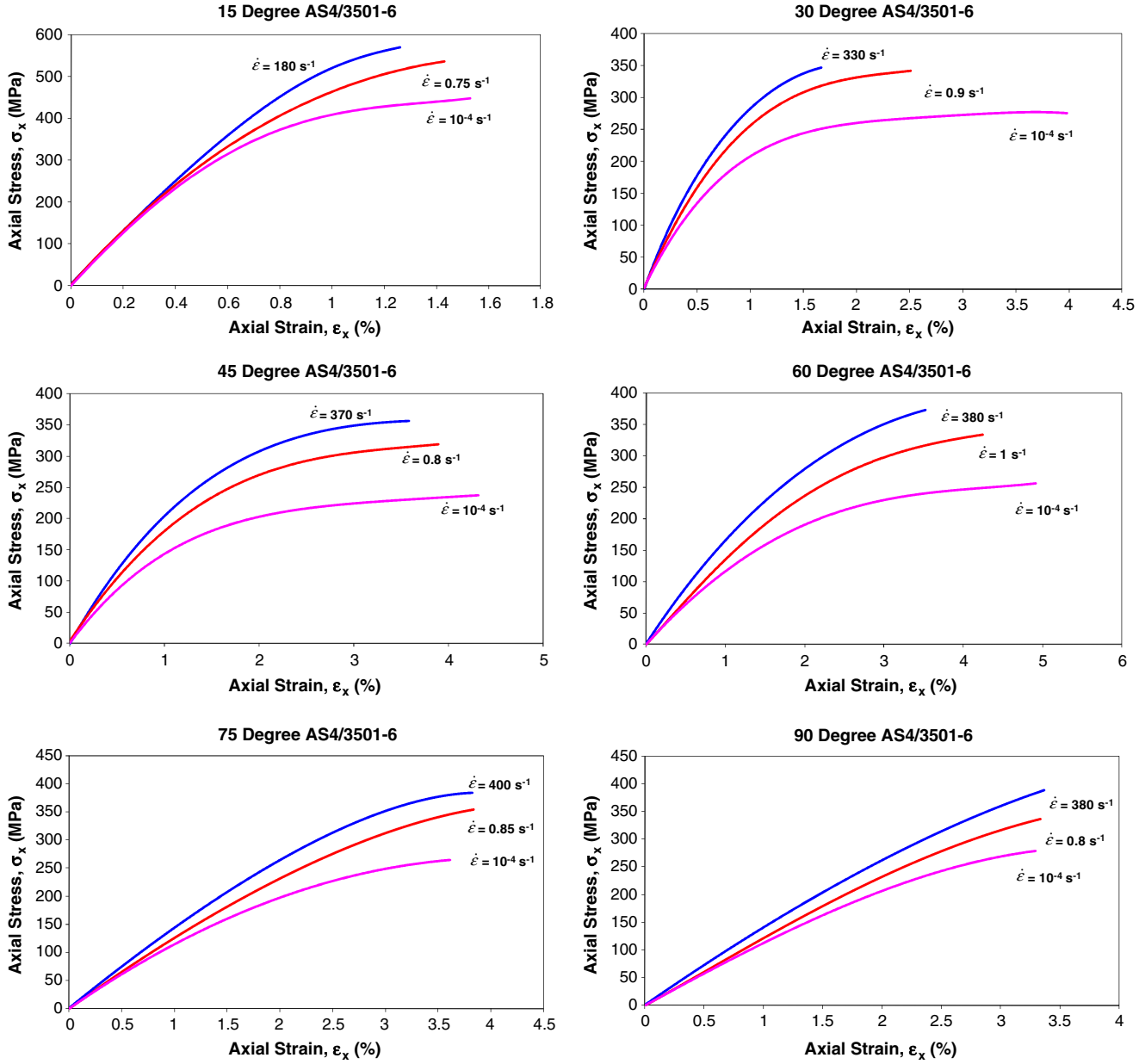

Fig. 3 Static and dynamic stress–strain curves for unidirectional carbon/epoxy composite under compressive loading at various orientations with the fiber direction.

dilatational deformation components. The proposed model describes the multi-axial stress–strain behavior measured at various strain rates and accounts for the sign of the normal stress (tension or compression). A general three-dimensional potential function f or effective stress $\bar{\sigma}_e$ was formulated for a transversely isotropic composite by taking the positive square root of Chen and Sun's [18] potential function and adding a term with a linear combination of normal stresses as

$$f = \{a_1[(\sigma_1 - \mu\sigma_2)^2 + (\sigma_1 - \mu\sigma_3)^2] + a_2(\sigma_2 - \sigma_3)^2 + a_4\tau_4^2 + a_6(\tau_5^2 + \tau_6^2)\}^{\frac{1}{2}} + [b_1\sigma_1 + b_2(\sigma_2 + \sigma_3)] = \bar{\sigma}_e \quad (3)$$

where a_1, a_2, a_4, a_6, b_1, and b_2 are plastic anisotropy parameters. The first bracketed term in Eq. (3) is related to shear deformation, and the second (linear) term is related to dilatational deformation. The parameter μ is an elastic anisotropy parameter coupling normal stresses along the 1 and 2 and 1 and 3 directions and is related to the material stiffnesses C_{ij} (in contracted notation, i.e., $i, j = 1, 2, \ldots, 6$) as [18]

$$\mu = \frac{C_{11} + C_{12} + C_{13}}{C_{12} + C_{22} + C_{23}} = \frac{C_{11} + C_{12} + C_{13}}{C_{13} + C_{23} + C_{33}} \quad (4)$$

For a two-dimensional state of stress, with $\sigma_3 = \tau_4 = \tau_5 = 0$, the above expression for the effective stress, or loading function f, is reduced to

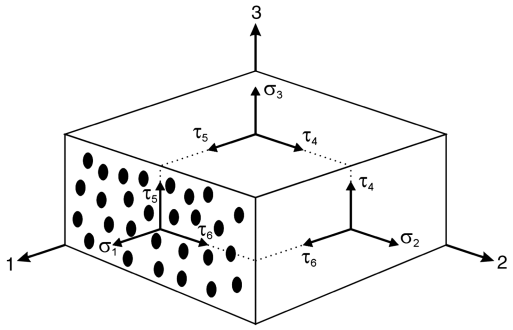

Fig. 4 Unidirectional composite element under load along the principal material axes.

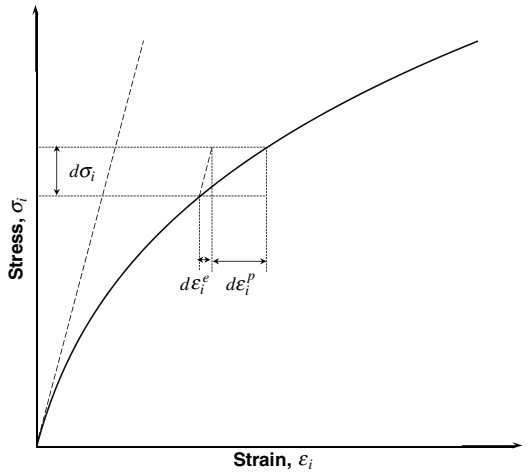

Fig. 5 Decomposition of strain increment in nonlinear elastic–plastic deformation.

$$f = \{a_1[(\sigma_1 - \mu\sigma_2)^2 + \sigma_1^2] + a_2\sigma_2^2 + a_6\tau_6^2\}^{\frac{1}{2}} + [b_1\sigma_1 + b_2\sigma_2] = \bar{\sigma}_e \tag{5}$$

The incremental stress–strain relation is

$$d\varepsilon_i = S_{ij}d\sigma_j + d\varepsilon_i^p \tag{6}$$

where S_{ij} is the material compliance tensor ($i, j = 1, 2, \ldots, 6$).

The incremental plastic strain energy per unit volume is given in terms of the effective plastic strain as

$$dW_p = \sigma_i d\varepsilon_i^p = \bar{\sigma}_e d\bar{\varepsilon}_p \tag{7}$$

where $d\bar{\varepsilon}_p$ is the increment in the effective plastic strain. Replacing the plastic strain increment with the gradient of the potential function by the flow rule (2),

$$\bar{\sigma}_e d\bar{\varepsilon}_p = \sigma_i \frac{\partial f}{\partial \sigma_i} d\lambda = \bar{\sigma}_e d\lambda \tag{8}$$

Therefore, the scalar function of proportionality is given by

$$d\lambda = d\bar{\varepsilon}_p \tag{9}$$

Assuming a power law relation between the effective plastic strain and effective stress as

$$\bar{\varepsilon}_p = A\bar{\sigma}_e^n \tag{10}$$

where A and n are functions of strain rate, we obtain the following expression for the scalar function:

$$d\lambda = nA(\bar{\sigma}_e)^{n-1}d\bar{\sigma}_e \tag{11}$$

The incremental effective stress, as defined in Eq. (5), is

$$d\bar{\sigma}_e = \frac{\partial f}{\partial \sigma_j} d\sigma_j \tag{12}$$

Using Eqs. (6), (2), and (9–12) we obtain the constitutive elasto/viscoplastic model for the total strain and stress increments as

$$d\varepsilon_i = \left[S_{ij} - nA\bar{\sigma}_e^{n-1}\frac{\partial f}{\partial \sigma_i}\frac{\partial f}{\partial \sigma_j}\right]d\sigma_j \tag{13}$$

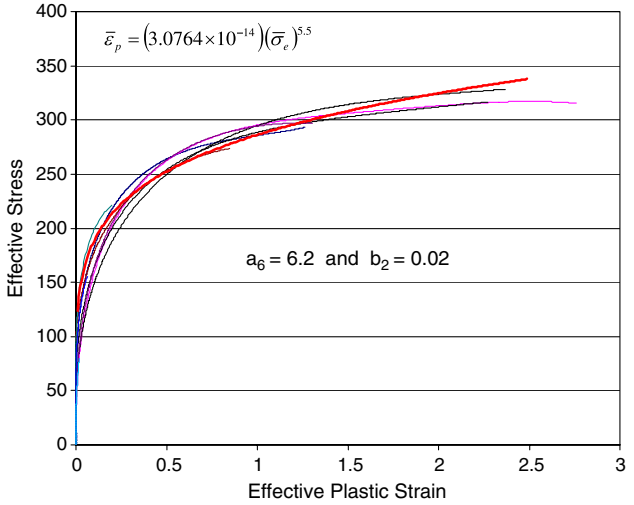

Fig. 6 Effective stress versus effective plastic strain fitted to experimental results for various loading conditions and strain rates with one set of constants (the parameters A and n vary with strain rate; the specific values in the inserted equation apply only for the 10^{-4} s^{-1} strain rate).

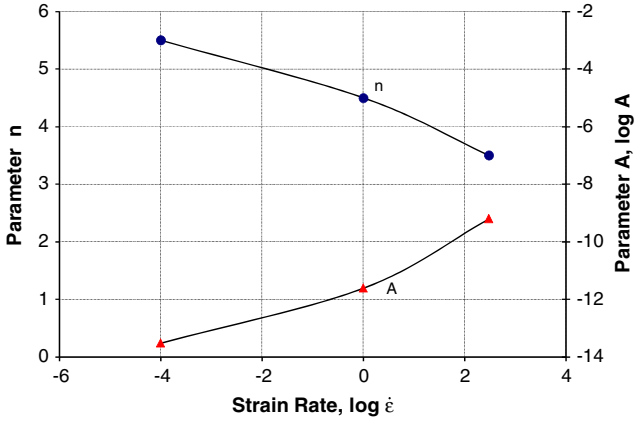

Fig. 7 Variation of model parameters with strain rate.

The yield criterion, assuming no plastic deformation in the fiber direction,

$$d\varepsilon_1^p = d\lambda\frac{\partial f}{\partial \sigma_1} = 0 \tag{14}$$

yields $a_1 = b_1 = 0$, and the potential function, after normalizing by a_2, is simplified as

$$f = \bar{\sigma}_e = [\sigma_2^2 + a_6\tau_6^2]^{\frac{1}{2}} + b_2\sigma_2 \tag{15}$$

IV. Experimental Model Validation

The model was validated experimentally for various states of biaxiality, tension, and compression and varying strain rates. The model parameters were determined from offaxis tension and compression tests, which provide various biaxial states of stress.

Table 1 Model parameters

Strain rate, s^{-1}	a_6	b_2	A, MPa$^{(-n)}$	n
0.0001	6.2	0.02	$3.0764 \times 10^{(-14)}$	5.5
1	6.2	0.02	$2.5165 \times 10^{(-12)}$	4.5
300	6.2	0.02	$6.4329 \times 10^{(-10)}$	3.5

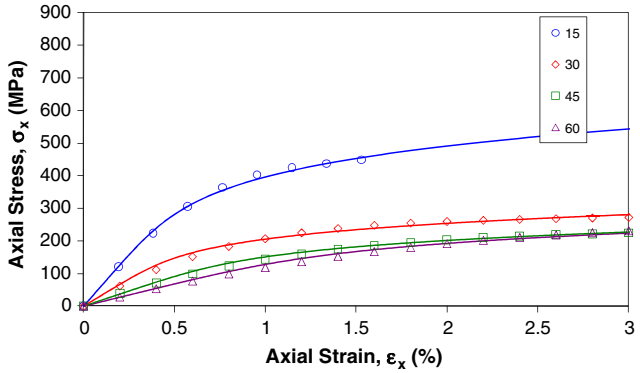

Fig. 8 Stress–strain curves under compression at various orientations with the fiber direction for quasi-static loading (solid curves represent model predictions).

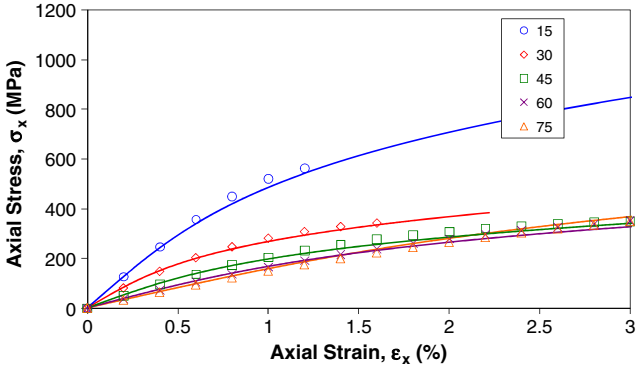

Fig. 9 Stress–strain curves under compression at various orientations with the fiber direction for high strain rate (solid curves represent model predictions).

Measured axial stresses and strains from the tests were related to the stress and strain components along the principal material directions by coordinate transformation. The stress components along the principal material axes are obtained in terms of the measured axial stress σ_x as

$$\sigma_1 = \sigma_x \cos^2\theta, \qquad \sigma_2 = \sigma_x \sin^2\theta, \qquad \tau_6 = -\sigma_x \sin\theta\cos\theta \quad (16)$$

where θ is the angle measured from the x axis (loading direction) to the 1-axis (fiber direction).

From Eq. (15) we obtain for tensile loading,

$$\bar{\sigma}_e = [(\sin^4\theta + a_6 \sin^2\theta\cos^2\theta)^{\frac{1}{2}} + b_2 \sin^2\theta]\sigma_x \quad (17)$$

and for compressive loading,

$$\bar{\sigma}_e = -[(\sin^4\theta + a_6 \sin^2\theta\cos^2\theta)^{\frac{1}{2}} - b_2 \sin^2\theta]\sigma_x \quad (18)$$

Similarly, the incremental plastic strain along the loading axis can be expressed in terms of its components along the principal material axes as

$$d\varepsilon_x^p = d\varepsilon_2^p \sin^2\theta - d\gamma_6^p \sin\theta\cos\theta \quad (19)$$

Substituting this plastic strain increment in Eq. (7) and integrating (for proportional loading), we obtain the effective plastic strain for tensile loading,

$$\bar{\varepsilon}_p = \frac{\sigma_x}{\bar{\sigma}_e}\varepsilon_x^p = [(\sin^4\theta + a_6 \sin^2\theta\cos^2\theta)^{\frac{1}{2}} + b_2 \sin^2\theta]^{-1}\varepsilon_x^p \quad (20)$$

and for compressive loading,

$$\bar{\varepsilon}_p = \frac{\sigma_x}{\bar{\sigma}_e}\varepsilon_x^p = -[(\sin^4\theta + a_6 \sin^2\theta\cos^2\theta)^{\frac{1}{2}} - b_2 \sin^2\theta]^{-1}\varepsilon_x^p \quad (21)$$

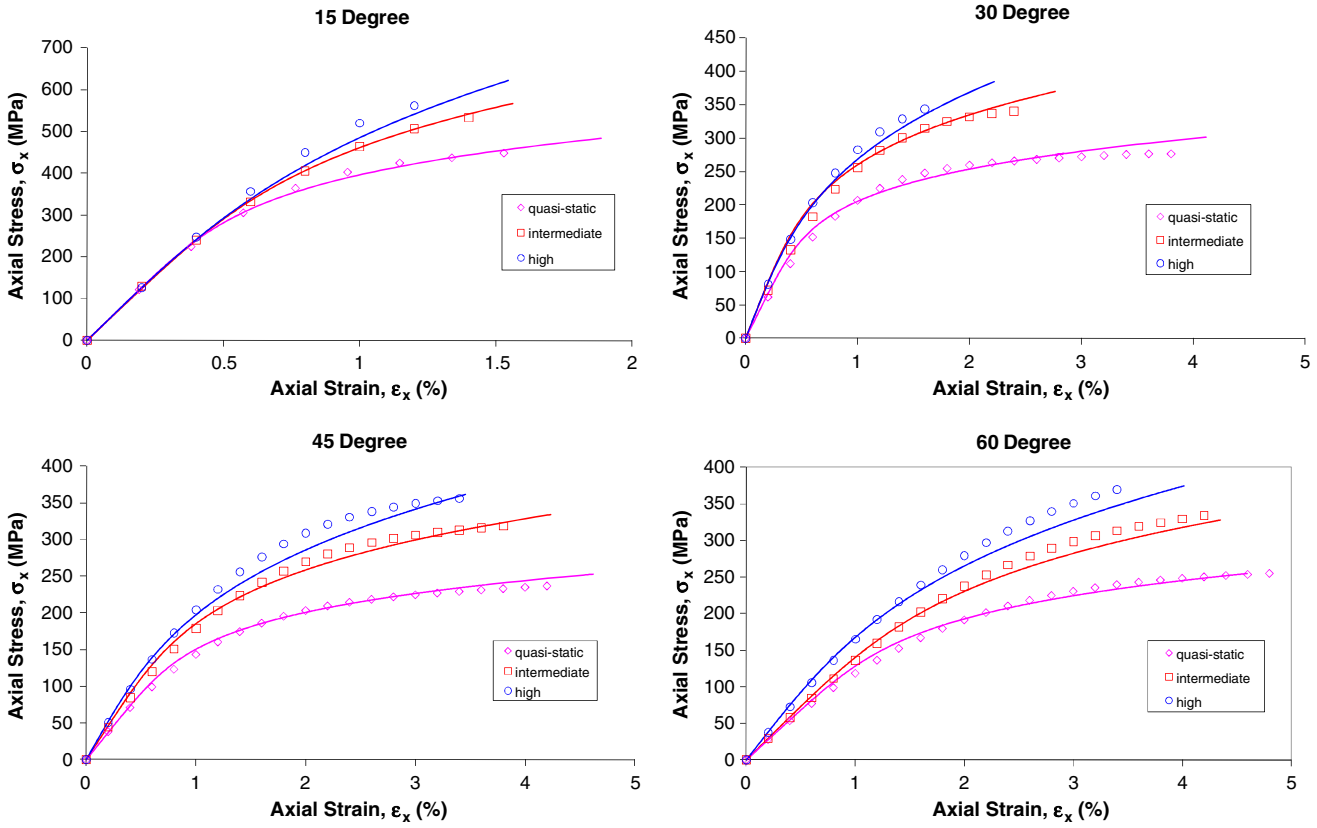

Fig. 10 Comparison of predicted and experimental stress–strain curves for carbon/epoxy composite loaded in compression at various orientations with the fiber direction at three strain rates (solid curves represent model predictions).

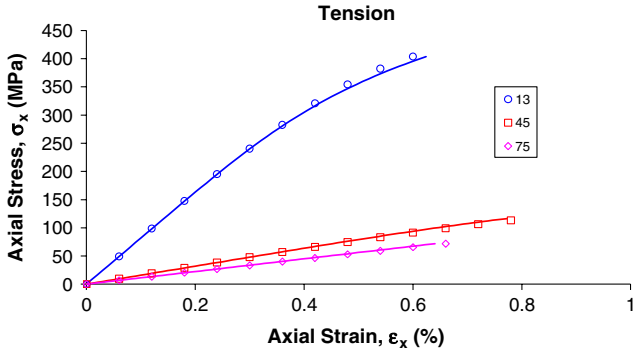

Fig. 11 Comparison of predicted and experimental stress–strain curves for carbon/epoxy composite loaded in tension at various orientations with the fiber direction (solid curves represent model predictions).

The above relations between effective stress and effective plastic strain were fitted to the experimental stress–strain curves shown in Fig. 3 for the carbon/epoxy composite. As shown in Fig. 6, all effective stress versus effective plastic strain curves for all loading conditions and strain rates covered by the experiments collapse into one curve for one set of constants, $a_6 = 6.2$ and $b_2 = 0.02$. The power law constants of A and n of Eq. (10) were determined by fitting the experimental data obtained and were found to be rate-dependent. Their variation with strain rate is shown in Fig. 7. The model constants for the three rates used in the experiments are tabulated in Table 1.

Comparisons of model predictions and experimental stress–strain curves under offaxis compression are shown in Figs. 8 and 9 for quasi-static and high-strain-rate loading. Similar comparisons between model predictions and experimental results are shown in Fig. 10 for the three strain rates investigated. A similar comparison for tensile loading at various orientations is shown in Fig. 11. A direct comparison between measured and predicted stress–strain curves in tension and compression is shown in Fig. 12 for two different loading orientations. In all cases the agreement between the model predictions and experimental results is very satisfactory.

V. Conclusions

A unidirectional carbon/epoxy composite was characterized at three strain rates, quasi-static (10^{-4} s^{-1}), intermediate (1 s^{-1}), and high (180–400 s^{-1}), under various biaxial states of stress combining transverse compression, tension, and shear. Stress–strain behavior was obtained under various biaxial states of stress at three strain rates by testing offaxis specimens under tension and compression. A two-parameter nonlinear constitutive model incorporating strain-rate dependence was proposed. The plastic potential function used in the model consists of decoupled shear and dilatation terms and thus distinguishes the sign of the normal stress component (tension or compression). The agreement between model predictions and experimental results is very satisfactory and shows that the proposed model is robust and is valid for both tension and compression under varying strain rates. The proposed model is not limited to the particular composite system tested, but can be applied to many other composite materials.

Acknowledgments

The work described in this paper was sponsored by the U.S. Office of Naval Research (ONR). We are grateful to Y. D. S. Rajapakse of the ONR for his encouragement and cooperation.

References

[1] Daniel, I. M., LaBedz, R., and Liber, T., "New Method for Testing Composites at Very High Strain Rates," *Experimental Mechanics*, Vol. 21, No. 2, 1981, pp. 71–77. doi:10.1007/BF02325199

[2] Daniel, I. M., Hamilton, W. G., and LaBedz, R. H., "Strain Rate Characterization of Unidirectional Graphite/Epoxy Composite," *Composite Materials: Testing and Design (Sixth Conference)*, ASTM STP 787, edited by I. M. Daniel, American Society for Testing and Materials, Philadelphia, 1982, pp. 393–413.

[3] Daniel, I. M., and LaBedz, R. H., "Method for Compression Testing at High Strain Rates," *Compression Testing of Homogeneous Materials and Composites*, ASTM STP 808, edited by R. Chait and R. Papirno, American Society for Testing and Materials, Philadelphia, 1983, pp. 121–139.

[4] Sierakowski, R. L., and Chaturvedi, S. K., *Dynamic Loading and Characterization of Fiber Reinforced Composites*, Wiley, New York, 1997.

[5] Hsiao, H. M., Daniel, I. M., and Cordes, R. D., "Dynamic Compressive Behavior of Thick Composite Materials," *Experimental Mechanics*, Vol. 38, 1998, pp. 172–180. doi:10.1007/BF02325740

[6] Hsiao, H. M., and Daniel, I. M., "Strain Rate Behavior of Composite Materials," *Composites, Part B*, Vol. 29, 1998, pp. 521–533. doi:10.1016/S1359-8368(98)00008-0

[7] Hsiao, H. M., Daniel, I. M., and Cordes, R. D., "Strain Rate Effects on the Transverse Compressive and Shear Behavior of Unidirectional Composites," *Journal of Composite Materials*, Vol. 33, 1999, pp. 1629–1642. doi:10.1177/002199839903301703

[8] Li, Z., and Lambros, J., "Determination of the Dynamic Response of Brittle Composites by the Use of the Split Hopkinson Pressure Bar," *Composites Science and Technology*, Vol. 59, 1999, pp. 1097–1107. doi:10.1016/S0266-3538(98)00152-3

[9] Woldesembet, E., and Vinson, J. R., "Specimen Geometry Effects on High-Strain Rate Testing of Graphite/Epoxy Composites," *AIAA Journal*, Vol. 37, No. 9, 1999, pp. 1102–1106. doi:10.2514/2.820

[10] Vinson, J. R., and Woldesenbet, E., "Fiber Orientation Effects on High Strain Rate Properties of Graphite/Epoxy Composites," *Journal of Composite Materials*, Vol. 35, 2001, pp. 509–521. doi:10.1177/002199801772662136

[11] Ninan, L., Tsai, J., and Sun, C. T., "Use of Split Hopkinson Pressure Bar for Testing offaxis Composites," *International Journal of Impact Engineering*, Vol. 25, 2001, pp. 291–313. doi:10.1016/S0734-743X(00)00039-7

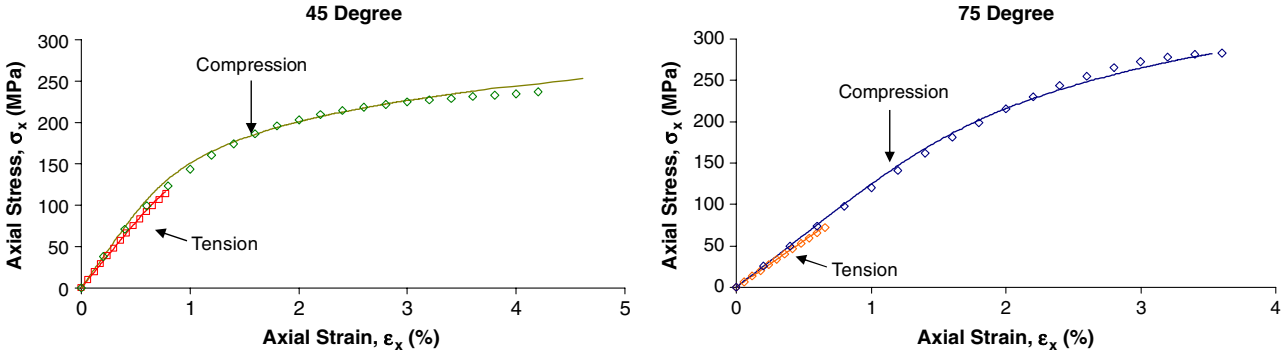

Fig. 12 Experimental and predicted stress–strain curves in tension and compression for two offaxis specimens (solid curves represent model predictions).

[12] Gilat, A., Goldberg, R. K., and Roberts, G. D., "Experimental Study of Strain-Rate-Dependent Behavior of Carbon/Epoxy Composite," *Composites Science and Technology*, Vol. 62, 2002, pp. 1469–1476. doi:10.1016/S0266-3538(02)00100-8

[13] Bing, Q., and Sun, C. T., "Modeling and Testing Strain Rate-Dependent Compressive Strength of Carbon/Epoxy Composites," *Composites Science and Technology*, Vol. 65, 2005, pp. 2481–2491. doi:10.1016/j.compscitech.2005.06.012

[14] Sun, C. T., and Chen, J. L., "A Simple Flow Rule for Characterizing Nonlinear Behavior of Fiber Composites," *Journal of Composite Materials*, Vol. 23, 1989, pp. 1009–1020. doi:10.1177/002199838902301004

[15] Gates, T. S., and Sun, C. T., "Elastic/Viscoplastic Constitutive Model for Fiber Reinforced Thermoplastic Composites," *AIAA Journal*, Vol. 29, No. 3, 1991, pp. 457–463. doi:10.2514/3.59922

[16] Hill, R., *The Mathematical Theory of Plasticity*, Oxford Univ. Press, London, 1950.

[17] Winn, V. M., and Sridharan, S., "An Investigation into the Accuracy of a One-parameter Nonlinear Model for Unidirectional Composites," *Journal of Composite Materials*, Vol. 35, No. 16, 2001, pp. 1491–1507. doi:10.1106/M99D-14RL-NHHF-CHWN

[18] Chen, J. L., and Sun, C. T., "A Plastic Potential Function Suitable for Anisotropic Fiber Composites," *Journal of Composite Materials*, Vol. 27, No. 14, 1993, pp. 1379–1390. doi:10.1177/002199839302701403

[19] Yokozeki, T., Ogihara, S., Yoshida, S., and Ogasawara, T., "Simple Constitutive Model for Nonlinear Response of Fiber-Reinforced Composites with Loading-Directional Dependence," *Composites Science and Technology*, Vol. 67, 2007, pp. 111–118. doi:10.1016/j.compscitech.2006.03.024

[20] Drucker, D. C., and Prager, W., "Soil Mechanics and Plastic Analysis or Limit Design," *Quarterly of Applied Mathematics*, Vol. 10, 1952, pp. 157–165.

[21] Thiruppukuzhi, S. V., and Sun, C. T., "Testing and Modeling High Strain Rate Behavior of Polymeric Composites," *Composites, Part B*, Vol. 29, 1998, pp. 535–546. doi:10.1016/S1359-8368(98)00009-2

[22] Thiruppukuzhi, S. V., and Sun, C. T., "Models for the Strain-Rate-Dependent Behavior of Polymer Composites," *Composites Science and Technology*, Vol. 61, 2001, pp. 1–12. doi:10.1016/S0266-3538(00)00133-0

[23] Weeks, C. A., and Sun, C. T., "Modeling Non-Linear Rate-Dependent Behavior in Fiber-Reinforced Composites," *Composites Science and Technology*, Vol. 58, 1998, pp. 603–611. doi:10.1016/S0266-3538(97)00183-8

[24] Goldberg, R. K., and Stouffer, D. C., "Strain Rate Dependent Analysis of a Polymer Matrix Composite Utilizing a Micromechanics Approach," *Journal of Composite Materials*, Vol. 36, 2002, pp. 773–793. doi:10.1177/0021998302036007613

[25] Zhu, L. F., Kim, H. S., Chattopadhyay, A., and Goldberg, R. K., "Improved Transverse Shear Calculations for Rate-Dependent Analyses of Polymer Matrix Composites," *AIAA Journal*, Vol. 43, No. 4, 2005, pp. 895–905. doi:10.2514/1.11793

[26] Xing, L., and Reifsnider, K. L., "Progressive Failure Modeling for Dynamic Loading of Woven Composites," *Applied Composite Materials*, Vol. 15, 2008, pp. 1–11. doi:10.1007/s10443-008-9053-7

[27] Donadon, M. V., de Almeida, S. F. M., Arbelo, M. A., and de Faria, A. R., "A Three-Dimensional Ply Failure Model for Composite Structures," *International Journal of Aerospace Engineering*, 2009, Paper 486063. doi:10.1155/2009/486063.

A. Pelegri
Associate Editor